
Generative Model for Synthesizing Ionizable Lipids: A Monte Carlo Tree Search Approach

Jingyi Zhao

Department of Engineering
University of Cambridge
Cambridge, CB2 1PZ
jz610@cam.ac.uk

Yuxuan Ou

Department of Engineering
University of Cambridge
Cambridge, CB2 1PZ
yuxuan.ou@trinity.ox.ac.uk

Austin Tripp

Department of Engineering
University of Cambridge
Cambridge, CB2 1PZ
ajt212@cam.ac.uk

Morteza Rasoulianboroujeni

School of Pharmacy
University of Wisconsin-Madison
Madison, WI 53705
rasoulianbor@wisc.edu

José Miguel Hernández-Lobato

Department of Engineering
University of Cambridge
Cambridge, CB2 1PZ
jmh233@cam.ac.uk

Abstract

Ionizable lipids are essential in developing lipid nanoparticles (LNPs) for effective messenger RNA (mRNA) delivery. While traditional methods for designing new ionizable lipids are typically time-consuming, deep generative models have emerged as a powerful solution, significantly accelerating the molecular discovery process. However, a practical challenge arises as the molecular structures generated can often be difficult or infeasible to synthesize. This project explores Monte Carlo tree search (MCTS)-based generative models for synthesizable ionizable lipids. Leveraging a synthetically accessible lipid building block dataset and two specialized predictors to guide the search through chemical space, we introduce a policy network guided MCTS generative model capable of producing new ionizable lipids with available synthesis pathways.

1 Introduction

The development of messenger RNA (mRNA)-based therapeutics marks a transformative advance in the treatment and prevention of a wide range of diseases, including genetic disorders, infectious diseases, and cancer [Sahin et al., 2014, Kong et al., 2023]. Given the intrinsic instability of mRNA, a robust delivery mechanism is crucial, with ionizable lipid nanoparticles (LNPs) emerging as the leading technology for this purpose [Mitchell et al., 2021, Kularatne et al., 2022]. These LNPs comprise four distinct lipid types, among which the ionizable amine-containing lipids are pivotal. They primarily facilitate the encapsulation of mRNA within LNPs and enhance its delivery into the cellular cytoplasm, where it can be translated into therapeutic proteins [Kim et al., 2021, Degors et al., 2019, Wittrup et al., 2015, Xu et al., 2021]. Notably, different LNPs often feature unique ionizable lipid structures, emphasizing the importance of developing a diverse array of ionizable lipids. This diversity is crucial for effectively delivering mRNA to various target cells and tissues, highlighting the need for continued innovation in the design of ionizable lipids to facilitate mRNA-based therapeutics.

Designing novel ionizable lipids is traditionally time-consuming and labor-intensive. However, recent advancements in the integration of deep learning with combinatorial chemistry have shown great promise in accelerating this development [Xu et al., 2024]. One of the primary challenges in ionizable lipid generation is the effective exploration of a vast combinatorial chemical space. The SyntheMol approach has demonstrated considerable success in this area, utilizing Monte Carlo tree search

(MCTS) to efficiently navigate through expansive search spaces and generate desired molecules, complete with synthesis pathways, particularly in the field of antibiotic development [Swanson et al., 2024].

This work extends the application of the MCTS-based generative model to the domain of ionizable lipid generation. We introduce a policy network guided MCTS method which leverages the strengths of MCTS and integrates it with the strategic direction provided by the policy network, aiming to optimize the generation process and yield new ionizable lipids more efficiently. Our main contributions are:

- We compile a synthetically accessible dataset of molecules suitable for use as ionizable lipid heads or lipid tails, which can facilitate future ionizable lipid generation tasks.
- We develop reliable lipid property predictors to assess whether a candidate molecule possesses lipid-like characteristics or ionizable properties.
- We propose and implement a generative model that leverages a policy network to guide the MCTS in exploring the chemical space. This model effectively generates high-quality products, complete with available synthesis pathways.

2 Related Work

Deep generative models have emerged as a powerful solution to the inverse molecular design challenge, enabling the translation of desired molecular properties into specific molecular structures [Kusner et al., 2017, Gómez-Bombarelli et al., 2018, Simonovsky and Komodakis, 2018, Assouel et al., 2018, Bian et al., 2019, Shi et al., 2021, Luo et al., 2021]. A practical problem that obstructs the usefulness of these generative algorithms is that proposed molecular structures may be challenging or infeasible to synthesize [Gao and Coley, 2020]. While post-hoc synthesis planning for generated molecules is feasible [Gao and Coley, 2020, Segler et al., 2017, 2018], a more effective approach is to incorporate synthesis instructions directly into the design phase. One effective solution is to adopt a bottom-up approach which begins with existing building blocks and strategically determines pathways to synthesize product molecules possessing desired properties [Bradshaw et al., 2020, Swanson et al., 2024].

Identifying new ionizable lipids remains a bottleneck of LNP development. Current state-of-the-art approaches still primarily rely on combinatorial chemistry techniques. Even when synthesized, an ionizable lipid often fails to exhibit transfection capabilities, with a low likelihood of achieving high transfection efficiency [Xu et al., 2024, Li et al., 2024]. Despite the vast structural design space of ionizable lipids, small modifications in chemical structure can lead to substantial differences in biological performance [Li et al., 2024]. Existing approaches that incorporate machine learning into ionizable lipid development primarily focus on building transfection efficiency predictors to aid in lipid screening [Xu et al., 2024, Li et al., 2024, Ding et al., 2023, Moayedpour et al., 2024]. However, no current approaches directly utilize machine learning for the generative design of ionizable lipids.

3 Background

This section presents the theoretical background of this work.

3.1 Monte Carlo Tree Search in Molecular Generation

MCTS is a robust algorithm that integrates the stochastic nature of Monte Carlo simulations with the structured decision-making processes inherent in tree searches [Kocsis and Szepesvari, 2006, Coulom, 2006]. A recent study has shown that MCTS-based generative models can perform successfully in small-molecule antibiotic development [Swanson et al., 2024]. In the context of SyntheMol, the algorithm iteratively builds a tree structure, where each node represents one or more potential molecular structures, and branches represent possible synthesis steps using 13 well-validated chemical reactions [Swanson et al., 2024]. The application of SyntheMol to lipid generation is detailed in Appendix B.

3.2 Guided Monte Carlo Tree Search

The pioneering work that integrates neural networks with MCTS is AlphaGo [Silver et al., 2016]. Building upon that, AlphaZero refined this approach by merging the policy and value networks into a single, more efficient neural network [Silver et al., 2017]. What's more, AlphaZero was trained exclusively through self-play, enabling the system to adapt and optimize its game play without relying on external data. AlphaZero provides a highly relevant framework for the application to molecular generation. Although our approach diverges from AlphaZero in that it does not integrate a value network within the MCTS framework—instead relying on separate property predictors—the role of the policy network remains pivotal in both contexts. In molecular generation, our policy network is instrumental in selecting the next building block for synthesis, which directly influences the structure and properties of the resultant molecule, akin to how each move in Go influences the progression and outcome of the game.

3.3 Retrosynthesis Evaluation

While the ideal method to validate the synthesis pathway of our generated products would be through experimental testing in a laboratory, practical constraints currently prevent us from doing so. Consequently, we rely on in silico evaluations to estimate synthesizability. We first calculate the synthetic accessibility score (SA score) to predict synthesizability in an automated manner [Ertl and Schuffenhauer, 2009]. Additionally, we seek to validate our proposed synthesis pathways using Syntheseus [Maziarz et al., 2023], a python package for retrosynthetic planning.

The SA score is calculated through a combination of fragment contributions and a complexity penalty [Ertl and Schuffenhauer, 2009]. The resulting SA score provides a metric for synthetic accessibility, ranging from 1 (indicating easy synthesis) to 10 (indicating high difficulty). However, while the SA score differentiates between feasible and infeasible molecules to some extent, it does not provide specific insights into the actual synthesis pathways. Syntheseus operates by recursively decomposing a target molecule into increasingly simpler molecules through a backward reaction prediction model, continuing until it identifies a set of synthetically accessible building blocks [Maziarz et al., 2023]. In our experiments, we employ the Molecule Edit Graph Attention Network (MEGAN) backward reaction prediction model [Sacha et al., 2020].

4 Methodology

This section presents the lipid building block dataset construction, the lipid property predictors, the reaction prediction model, and the policy network guided MCTS approach for lipid generation.

4.1 Dataset Construction

An ionizable lipid consists of an ionizable lipid head and several lipid tails. Our building block datasets contain synthetically accessible molecules that can act as lipid heads or lipid tails. We filter valid lipid building blocks from the ZINC20 database [Irwin et al., 2020], a large-scale chemical database designed for drug discovery and virtual screening.

Figure 1 shows the flowcharts for constructing lipid head and lipid tail building block datasets. For the ionizable lipid head dataset, we first filter ionizable molecules from the ZINC20 molecule dataset based on specific criteria of LogP value, molecular weight, and amine groups. Since the lipid head building blocks are expected to react with lipid tail building blocks, we further filter reactive molecules by identifying whether or not the molecule contains certain functional groups that participate in common reactions. Detailed filtering criteria are presented in Appendix A.

We identify a lipid tail building block if the molecule is similar to an actual lipid tail (i.e., the tail component of an existing lipid). Taking advantage of the Lipid Analyzer¹, an implemented toolkit for lipid tail extraction, we extract lipid tails from a lipid dataset sourced from [Sud et al., 2007, Aimo et al., 2015]. We then conduct a similarity comparison to filter those molecules from the ZINC20 dataset that are similar to a real lipid tail. The resulting molecules make up our lipid tail building

¹The Lipid Analyzer toolkit is an unpublished work.

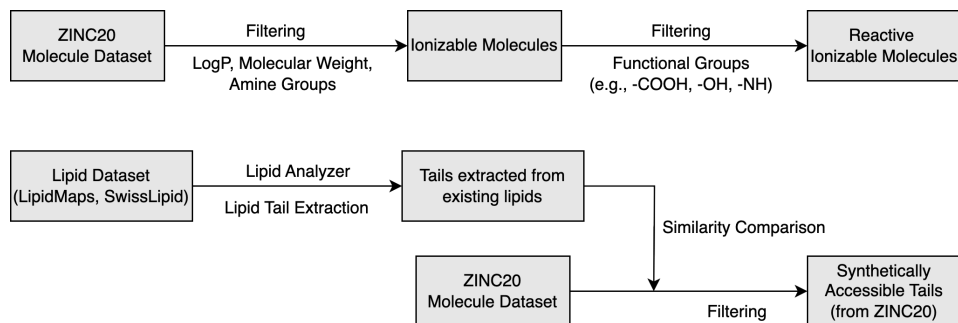


Figure 1: Roadmap of lipid building block datasets construction. The upper flowchart illustrates the process of filtering ionizable lipid head building block dataset. The lower flowchart illustrates the process of constructing lipid tail building block dataset.

block dataset. Detailed information of the dataset construction process and selective examples of lipid building blocks are shown in Appendix A.

4.2 Lipid Property Prediction

Our generative approach relies on molecular property predictors to evaluate the potential of generated molecules to be an ionizable lipid. We employ a lipid classifier for binary assessment of lipid-likeness and an ionizability predictor to evaluate whether the generated product is ionizable.

Lipid Classifier Utilizing the Chemprop graph neural network framework [Yang et al., 2019], our lipid classifier features three message passing layers that integrate molecular features, complemented by two feed-forward layers dedicated to predicting molecular properties. The dataset we use to train the lipid classifier contains 180 000 lipid samples and 180 000 non-lipid samples. The non-lipid samples are small molecules from the PubChem database [Kim et al., 2016]. Part of the lipid samples come from publicly accessible lipid dataset LipidMaps and SwissLipids [Sud et al., 2007, Aimo et al., 2015]. The rest of the lipid samples are generated using a hierarchical graph encoder-decoder that employs significantly large and flexible graph motifs as basic building blocks [Jin et al., 2020].

Ionizability Predictor An ionizable molecule has neutral charge in physiological pH and becomes positively charged in acidic environments [Carrasco et al., 2021, Stern and McNeil, 2007]. For simpler filtering purpose, we only consider the net charge under $\text{pH} = 7.4$ (i.e., represents the physiological pH) and $\text{pH} = 5$ (i.e., represents the acidic environment). We utilize the MolGpKa module to determine acidic and basic groups within a given molecule and to estimate their respective pKa values [Pan et al., 2021]. The net charge of each molecule under a given pH value can then be calculated using the Henderson-Hasselbalch equation [Petrucci et al., 2002].

4.3 Reaction Prediction

We employ a template-based reaction prediction model which applies predefined reaction templates—derived from known chemical reaction mechanisms—to reactants. The advantages of this approach include faster computation, adherence to established chemical rules, and higher synthesis success potential. We adopt the same reaction templates as SyntheMol, our baseline model. The combinatorial chemical space explored by SyntheMol was the Enamine REadily Accessible (REAL) Space [Grygorenko et al., 2020]. SyntheMol employs 13 reactions that account for 93.9% of the REAL Space [Swanson et al., 2024]. Although our lipid building block dataset differs from the REAL space, the selected reactions are widely applicable across a broad range of chemicals, making them suitable for our project as well.

4.4 Guided Monte Carlo Tree Search for Lipid Generation

Building upon the SyntheMol and inspired by AlphaZero [Swanson et al., 2024, Silver et al., 2017], we apply the policy network guided MCTS to ionizable lipid generation. The integration of a policy network with MCTS forms the cornerstone of our approach, enabling a strategic exploration of

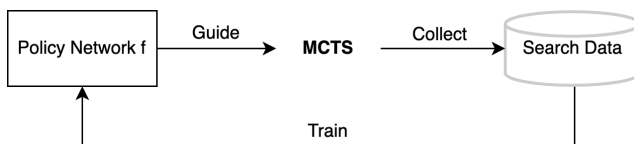


Figure 2: Workflow of policy network training.

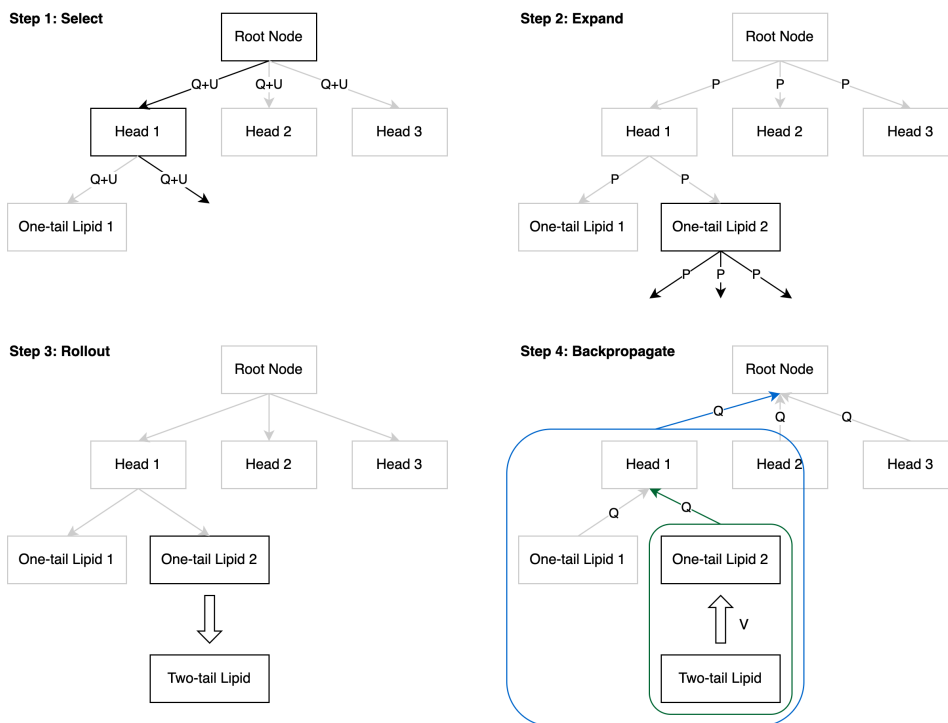


Figure 3: Policy network guided Monte Carlo tree search for lipid generation.

chemical spaces through guided decision-making. In our problem formulation, the state is defined as the current molecule, and the action as the selection of the next building block. The policy network assigns probabilities to potential actions for each state. The training of the policy network is a cyclic process, aimed at progressively improving the network’s ability to predict and prioritize effective synthetic pathways.

Figure 2 illustrates the workflow of the policy network training procedure. We start from a randomly initialized policy network which assigns equal probabilities to all the actions in the provided action space. This policy network will be used to guide the MCTS. We conduct the tree search for a number of simulations, and the search data (i.e., visit counts of all state-action pairs involved) of the tree search will be used as the training data to train the policy network for several epochs. We propose a customized policy network training technique, which is detailed in Appendix D. This process serves as one iteration of policy network training. In the next iteration, we use the updated policy network to guide MCTS and repeat the process.

A step-wise depiction of each simulation of the MCTS is shown in Figure 3, with the detailed algorithm presented in Appendix C. Each simulation of the MCTS consists of four steps: select, expand, rollout, and backpropagate. We define the policy network that guides the MCTS simulations to be f_θ with parameters θ . Each edge in the tree search represents a state-action pair (s, a) where state s is the current molecule we have and action a is the next building block molecule to choose. Each edge stores a set of statistics $\{N(s, a), W(s, a), P(s, a)\}$ where $N(s, a)$ is the visit count, $W(s, a)$ is the total action value (i.e., sum of values of final products reached after taking action a from state s), and $P(s, a)$ is the prior probability of selecting that edge. Note that $P(s, \cdot) = f_\theta(s)$ is given by the current policy network.

In the selection step, each simulation traverses the tree by selecting the edge with the maximum Upper Confidence Bound (UCB) score until a leaf node is reached. At each time step t , our action selection criterion follows

$$a_t = \arg \max_a UCB_score(s_t, a) = \arg \max_a (Q(s_t, a) + U(s_t, a)) \quad (1)$$

The UCB score is defined to be

$$UCB_score(s, a) = Q(s, a) + U(s, a) \quad (2)$$

$$= \frac{W(s, a)}{N(s, a)} + c \cdot P(s, a) \cdot \frac{\sqrt{\sum_b N(s, b)}}{1 + N(s, a)} \quad (3)$$

where c is a constant parameter controlling the level of exploration.

In the expansion step, the leaf node selected in the previous step will be expanded. First, the state s of the leaf node will be calculated as the chemical product of the state and action molecules represented by the edge which directs to this leaf node. We then find the action space $A(s)$ of the leaf node and calculate $P(s, a)$ values for all $a \in A(s)$ via the policy network, i.e., $P(s, \cdot) = f_\theta(s)$. The P values will be stored in the newly-added outgoing edges from the selected leaf node.

Meanwhile, the selected leaf node will be evaluated by the rollout step. This step aims to get a value for the selected leaf node. The rollout means performing random actions until we reach the end of the play (i.e., until we generate a two-tail lipid). This randomly generated product will be evaluated by the property predictor and this property score will act as the value of the selected leaf node.

Once we have the value of the selected leaf node, we perform the last step of the simulation, backpropagation. The value will be backpropagated along the chosen path to update action values Q .

5 Experiments

Our experimental investigation focuses on comparing the performance of the SyntheMol approach, served as the baseline, with our proposed policy network guided MCTS approach. We demonstrate the enhanced efficiency of the guided MCTS approach in identifying and synthesizing high-potential ionizable lipids.

5.1 Experimental Setups

Lipid Building Block Dataset Following the procedure described in Section 4.1, we construct a lipid building block dataset consisting of over 2.7 million lipid head building blocks and 5310 lipid tail building blocks. While directly incorporating such huge dataset into the MCTS would result in a predominantly exploratory behavior akin to random selections, we extract a subset of approximately 12 000 head building blocks to define our actual head search space. The entire tail building block dataset is utilized in subsequent levels of the search. For the evaluation of the policy network in the guided MCTS approach, an additional set of 200 testing head building blocks is employed.

SyntheMol Configuration We constrain the maximum number of child node expansions to be 2 000, meaning that each MCTS explores a head search space of this size. The MCTS is executed over 10 000 simulations to ensure comprehensive analysis of the generated lipid products. Additionally, the exploration weight c used in the UCB score calculation, as detailed in Equation 5, is set at 10.

Guided MCTS Configuration We operate the guided MCTS across 10 iterations. For every iteration, the MCTS is executed 10 times, each exploring a head space of 200. This setup allows the 10 runs of MCTS collectively to explore a total head search space size of 2 000, aligning with the head search space used in the SyntheMol approach. Each MCTS runs 10 000 simulations to gather substantial search data. The data from these 10 MCTS runs are pooled to train the policy network, and the accumulated generated products are analyzed as the iteration’s output. The policy network undergoes 20 epochs of training in each iteration. The exploration weight c used in the UCB score calculation, as outlined in Equation 2, is set at 20.

Policy Network Configuration The policy network processes state-action pairs, where each state is the current molecule and the action is the next building block molecule selected. Each molecule is represented using a Morgan fingerprint with 1024-bit binary digit and radius 2 [Schneider et al.,

2015], and the fingerprints of both the state and action molecules are concatenated to form a 2048-bit feature vector, serving as the input to the policy network. Our policy network architecture consists of four linear layers, each followed by a ReLU activation function [Fukushima, 1969] and dropout layers with a dropout rate of 0.5 [Wan et al., 2013] to prevent overfitting. The Adam optimizer is used for network training, with a learning rate of 0.001 [Kingma and Ba, 2017].

Computing Resources Our computational setup includes a GPU server equipped with 8 Tesla P-100 GPUs, each featuring 16 GB of memory. It is important to note that within our experimental framework, only the MolGpKa module is configured to utilize GPU resources [Pan et al., 2021]. All other components of our algorithms are designed to run efficiently on CPU.

5.2 Results and Discussions

We first present the performance of our lipid property predictors and then compare the generative results of the SyntheMol approach with our proposed policy network guided MCTS approach.

5.2.1 Lipid Property Prediction

As previously mentioned, we utilize a Chemprop based binary lipid classifier to determine whether a candidate molecule is lipid-like [Yang et al., 2019]. After training for a single epoch, our model demonstrates exceptional performance, achieving both Receiver Operating Characteristic Area Under the Curve (ROC-AUC) and Precision-Recall Area Under the Curve (PR-AUC) scores above 0.9999. Together, these metrics, along with a test accuracy of 99.89%, underscore the robustness and predictive accuracy of our lipid classifier.

In terms of ionizability, we utilize the MolGpKa module to identify ionizable groups within a target molecule and calculates their corresponding pKa values. We then determine the net charge of the target molecule at specific pH levels and conduct the ionizability filtering. According to [Pan et al., 2021], the MolGpKa predictor has undergone rigorous testing, thus justifying the credibility of our ionizability predictions.

To better validate our lipid property predictors, we curated an ionizable lipid dataset with more than 2 500 ionizable lipids that have been experimentally synthesized from published works [Xu et al., 2024, Li et al., 2023, He et al., 2023, Liu et al., 2021, Abd Elwakil et al., 2023, Yu et al., 2020, Wei et al., 2023]. We evaluated our predictors on this dataset, achieving an accuracy of 98.32% for our lipid classifier. Notably, all ionizable lipids were correctly classified by the ionizability predictor.

5.2.2 Generative Results

Our primary objective is to generate products that are potent candidates for ionizable lipids, meaning we aim for molecules with high property scores. We begin by examining the products generated via the SyntheMol approach, which serves as a baseline for comparing the performance enhancements achieved with the guided MCTS approach.

The property score combines a lipid classifier score, which typically hovers near 0 or 1, and a binary ionizability score. A property score approaching 2 typically identifies the molecule as a likely ionizable lipid. After conducting 10 000 simulations, a total of 16 477 two-tail lipids were generated. We observe that only 4513 of the 16 477 generated products are predicted to be ionizable lipids, providing an ionizable lipid rate at 0.2739. To evaluate the effectiveness of MCTS, we conducted experiments with random generation. Specifically, we generated 10 000 unique two-tail lipids through random combinations using the same lipid head and tail building block subsets, achieving an ionizable lipid rate of 0.1547. This result justifies the effectiveness of MCTS in guiding the generation of ionizable lipids.

We now turn our attention to the outcomes of the policy network guided MCTS approach. By comparing these results with those from the SyntheMol approach, we seek to illustrate the enhanced effectiveness of the policy network guided MCTS in producing ionizable lipids. We analyze the unique generated products from both training and testing simulations. The primary distinction between these simulations lies in their respective head building block search spaces. However, it is important to note that the selection of head molecules significantly influences the quality of the generated products. Nonetheless, observing the trend in quality changes within a specific head set, as

guided by different iterations of the policy network, can still effectively illustrate the efficiency and impact of policy network training.

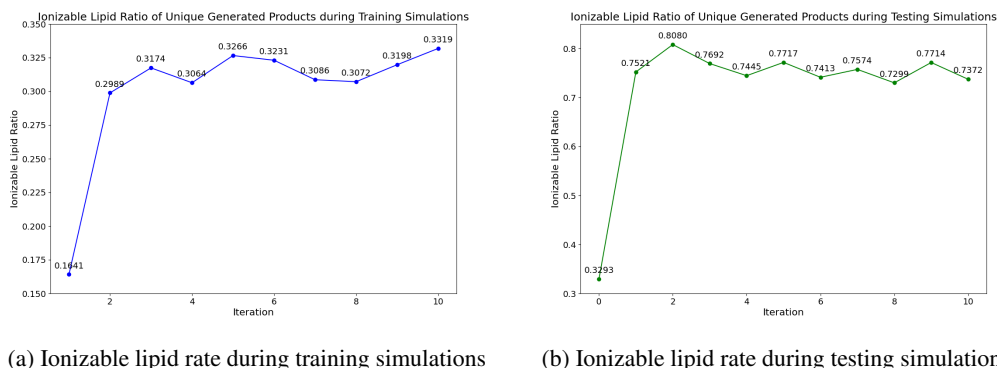


Figure 4: Ionizable lipid rate of the generated products during guided MCTS simulations.

Figure 4a depicts the ionizable lipid rate cross training iterations. The initial results in iteration 1 are derived from MCTS simulations guided by a randomly initialized policy network, whereas the results from iteration 2 onward are influenced by successively trained instances of the policy network. A distinct increase in the ionizable lipid generation rate is evident after the first training session, as is shown in Figure 4a, which underscores a significant enhancement in quality attributable to the training of the policy network, affirming its efficacy in refining the generation process. Figure 4b presents the ionizable lipid rate during testing simulations, each guided by policy networks trained across different iterations. The initial iteration (i.e., iteration 0) features products generated by MCTS simulations directed by a randomly initialized policy network, with subsequent iterations using progressively trained policy networks. The results demonstrate a marked improvement in the ionizable lipid rate following the initial training iteration. Subsequent iterations show the rate stabilizing, with only minor fluctuations observed, oscillating between 0.73 and 0.8. In either case, these rates significantly surpass the ionizable lipid rate of below 0.3 achieved by the SyntheMol approach, clearly demonstrating the superior performance of our model over the baseline. A detailed comparison of the ionizable lipid generation rate is presented in Table 1, where the rate for the guided MCTS corresponds to the value recorded after 10 iterations of policy network training.

5.2.3 Retrosynthesis Evaluation

Table 1 presents the evaluation results of our generated ionizable lipids and their corresponding synthesis pathways. We consider all unique products generated during both training and testing phases across all iterations of the guided MCTS approach. For better comparison, we also include the generated products from random combinations and the dataset of published ionizable lipids synthesized in previous works [Xu et al., 2024, Huayamares et al., 2023, Ly et al., 2022].

The SA score, which ranges from 1 to 10 with lower values indicating easier synthesis [Ertl and Schuffenhauer, 2009], reveals similar results for both the SyntheMol and guided MCTS approaches. Notably, there is no significant difference between the SA scores of our generated products and those of the published ionizable lipids. While the SA score justifies the synthesizability of the generated products to some extent, it does not offer any insights into their specific synthesis pathways.

Using Syntheseus, we aim to identify synthesis pathways for the generated products using a backward reaction prediction model. Given that a single generated product may have multiple possible synthesis pathways, we do not strictly adhere to those suggested by the generative model. Instead, we focus on identifying reactants for the generated products and checking whether these reactants are present in our lipid building block dataset. We record the proportion of generated products that can be synthesized using molecules from the building block dataset.

We observe that the retrosynthesis rate validated by Syntheseus is not high, with none of the cases exceeding 50%. The low rate may result from the unique characteristics of the lipid building block dataset and the reaction templates we adopted. For retrosynthesis planning, we utilize the MEGAN backward reaction prediction model trained on the USPTO-50k dataset [Sacha et al., 2020]. Our lipid

Table 1: Evaluation of generated products and synthesis pathways.

	No. Unique Ionizable Lipids	Unique Ionizable Lipid Rate	Average SA Score	Retro Valid Rate by Synthesus
Guided MCTS Train	5058	0.3319	4.62	0.4881
Guided MCTS Test	545	0.7372	4.24	0.2679
SyntheMol	4513	0.2739	4.77	0.2719
Random Combination	1547	0.1547	4.44	0.3103
Published Lipids	2563	/	4.12	0.0433

building block molecules may differ significantly from the reactants in the USPTO reactions, and our reaction templates may not align well with those in the USPTO dataset. Additionally, a lot of the reaction templates involve using linker molecules, while such reactions might not be present in the USPTO dataset. These mismatches make retrosynthesis planning challenging and contribute to the low retrosynthesis rate. Regarding the published ionizable lipids that have been experimentally synthesized, we observe a retrosynthesis valid rate below 5%. This is likely because these lipids were synthesized using building blocks outside our building block dataset. Our building block dataset may lack many structures not included in the ZINC dataset. Additionally, our choice of weight cutoff and restrictions on amine-containing structures during lipid head dataset construction further reduce the search space.

Selected examples of generated ionizable lipids, along with their synthesis pathways validated by the retrosynthesis tool, are presented in Appendix E.

6 Conclusion

In this work, we have explored the Monte Carlo tree search (MCTS)-based generative models for ionizable lipid generation. We constructed a lipid building block dataset, featuring synthetically accessible ionizable lipid heads and tails, which is well-suited for future lipid generation tasks. We developed two lipid property predictors: a lipid classifier and an ionizability predictor, both designed to accurately assess whether a candidate molecule is lipid-like or ionizable. Adapting the SyntheMol approach, originally utilized for antibiotic discovery, we tailored this method for lipid generation to serve as our baseline model. We further innovated by developing a policy network guided MCTS-based generative model which is capable of producing high-quality ionizable lipids with available synthesis paths, outperforming our baseline. Our achievements indicate that this project offers a promising direction for ionizable lipid generation, also contributing to the broader field of drug delivery.

Nonetheless, it is important to acknowledge that the work has its limitations. If condition allowed, we may conduct experimental validations of the existing reaction templates with lipid building blocks to ensure their applicability and efficiency in lipid synthesis. It will be helpful to develop and integrate additional reaction templates that are specific to lipid chemistry. To address the limitation of not having practical synthesis validations, future research should prioritize establishing collaborations with chemical laboratories. This will enable empirical testing and validation of the synthesized molecules, providing a direct assessment of their practical viability and safety. Develop or customize computer-aided retrosynthesis tools specifically for ionizable lipid generation can also be helpful.

Acknowledgments and Disclosure of Funding

The authors would like to thank Asal Mehradfar and Mohammad Shahab Sepehri for curating the lipid dataset used for training lipid classifier and for building the Lipid Analyzer toolkit.

References

Mahmoud M. Abd Elwakil, Ryota Suzuki, Alaa M. Khalifa, Rania M. Elshami, Takuya Isono, Yaser H.A. Elewa, Yusuke Sato, Takashi Nakamura, Toshifumi Satoh, and Hideyoshi Harashima. Harnessing topology and stereochemistry of glycidylamine-derived lipid nanoparticles for in vivo

- mrna delivery to immune cells in spleen and their application for cancer vaccination. *Advanced Functional Materials*, 33(45):2303795, 2023. doi: <https://doi.org/10.1002/adfm.202303795>. URL <https://onlinelibrary.wiley.com/doi/abs/10.1002/adfm.202303795>.
- Lucila Aimo, Robin Liechti, Nevila Hyka-Nouspikel, Anne Niknejad, Anne Gleizes, Lou Götz, Dmitry Kuznetsov, Fabrice P. A. David, F. Gisou van der Goot, Howard Riezman, Lydie Bouguéleret, Ioannis Xenarios, and Alan Bridge. The swisslipids knowledgebase for lipid biology. *Bioinformatics*, 31(17):2860–2866, 2015. doi: 10.1093/bioinformatics/btv285.
- Rim Assouel, Mohamed Ahmed, Marwin H. S. Segler, Amir Saffari, and Yoshua Bengio. Defactor: Differentiable edge factorization-based probabilistic graph generation. *CoRR*, abs/1811.09766, 2018. URL <http://arxiv.org/abs/1811.09766>.
- Yuemin Bian, Junmei Wang, Jaden Jungho Jun, and Xiang-Qun Xie. Deep convolutional generative adversarial network (dcGAN) models for screening and design of small molecules targeting cannabinoid receptors. *Molecular Pharmaceutics*, 16(11):4451–4460, 2019. ISSN 1543-8384. doi: 10.1021/acs.molpharmaceut.9b00500. URL <https://doi.org/10.1021/acs.molpharmaceut.9b00500>. Publisher: American Chemical Society.
- John Bradshaw, Brooks Paige, Matt J. Kusner, Marwin H. S. Segler, and José Miguel Hernández-Lobato. Barking up the right tree: an approach to search over molecule synthesis dags, 2020.
- Manuel J. Carrasco, Suman Alishetty, Mohamad-Gabriel Alameh, Hooda Said, Lacey Wright, Mikell Paige, Ousamah Soliman, Drew Weissman, Thomas E. Cleveland, Alexander Grishaev, and Michael D. Buschmann. Ionization and structural properties of mRNA lipid nanoparticles influence expression in intramuscular and intravascular administration. *Communications Biology*, 4(1):956, 2021. ISSN 2399-3642. doi: 10.1038/s42003-021-02441-2. URL <https://doi.org/10.1038/s42003-021-02441-2>.
- Rémi Coulom. Efficient selectivity and backup operators in monte-carlo tree search. In *Computers and Games*, 2006. URL <https://api.semanticscholar.org/CorpusID:16724115>.
- Isabelle M. S. Degors, Cuifeng Wang, Zia Ur Rehman, and Inge S. Zuhorn. Carriers break barriers in drug delivery: Endocytosis and endosomal escape of gene delivery vectors. *Accounts of Chemical Research*, 52(7):1750–1760, 2019. ISSN 0001-4842. doi: 10.1021/acs.accounts.9b00177. URL <https://doi.org/10.1021/acs.accounts.9b00177>. Publisher: American Chemical Society.
- Daisy Yi Ding, Yuhui Zhang, Yuan Jia, and Jiuzhi Sun. Machine learning-guided lipid nanoparticle design for mrna delivery, 2023. URL <https://arxiv.org/abs/2308.01402>.
- Peter Ertl and Ansgar Schuffenhauer. Estimation of synthetic accessibility score of drug-like molecules based on molecular complexity and fragment contributions. *Journal of Cheminformatics*, 1(1):8, 2009. ISSN 1758-2946. doi: 10.1186/1758-2946-1-8. URL <https://doi.org/10.1186/1758-2946-1-8>.
- Kunihiko Fukushima. Visual feature extraction by a multilayered network of analog threshold elements. *IEEE Trans. Syst. Sci. Cybern.*, 5:322–333, 1969. URL <https://api.semanticscholar.org/CorpusID:206799280>.
- Wenhao Gao and Connor W. Coley. The synthesizability of molecules proposed by generative models, 2020. URL <https://arxiv.org/abs/2002.07007>.
- Oleksandr O. Grygorenko, Dmytro S. Radchenko, Igor Dziuba, Alexander Chuprina, Kateryna E. Gubina, and Yurii S. Moroz. Generating multibillion chemical space of readily accessible screening compounds. *iScience*, 23(11):101681, 2020. doi: 10.1016/j.isci.2020.101681. Published correction appears in *iScience*. 2020 Dec 04;23(12):101873. doi: 10.1016/j.isci.2020.101873.
- Rafael Gómez-Bombarelli, Jennifer N. Wei, David Duvenaud, José Miguel Hernández-Lobato, Benjamín Sánchez-Lengeling, Dennis Sheberla, Jorge Aguilera-Iparraguirre, Timothy D. Hirzel, Ryan P. Adams, and Alán Aspuru-Guzik. Automatic chemical design using a data-driven continuous representation of molecules. *ACS Central Science*, 4(2):268–276, January 2018. ISSN 2374-7951. doi: 10.1021/acscentsci.7b00572. URL <http://dx.doi.org/10.1021/acscentsci.7b00572>.

- Zepeng He, Zhicheng Le, Yi Shi, Lixin Liu, Zhijia Liu, and Yongming Chen. A multidimensional approach to modulating ionizable lipids for high-performing and organ-selective mRNA delivery. *Angewandte Chemie International Edition*, 62(43):e202310401, 2023. doi: <https://doi.org/10.1002/anie.202310401>. URL <https://onlinelibrary.wiley.com/doi/abs/10.1002/anie.202310401>.
- Sebastian G. Huayamares, Melissa P. Lokugamage, Regina Rab, Alejandro J. Da Silva Sanchez, Hyejin Kim, Afsane Radmand, David Loughrey, Liming Lian, Yuning Hou, Bhagelu R. Achyut, Annette Ehrhardt, Jeong S. Hong, Cory D. Sago, Kalina Paunovska, Elisa Schrader Echeverri, Daryll Vanover, Philip J. Santangelo, Eric J. Sorscher, and James E. Dahlman. High-throughput screens identify a lipid nanoparticle that preferentially delivers mRNA to human tumors in vivo. *Journal of Controlled Release*, 357:394–403, 2023. ISSN 0168-3659. doi: <https://doi.org/10.1016/j.jconrel.2023.04.005>. URL <https://www.sciencedirect.com/science/article/pii/S0168365923002559>.
- John J. Irwin, Khanh G. Tang, Jennifer Young, Chinzorig Dandarchuluun, Benjamin R. Wong, Munkhzul Khurelbaatar, Yurii S. Moroz, John Mayfield, and Roger A. Sayle. ZINC20—a free ultralarge-scale chemical database for ligand discovery. *Journal of Chemical Information and Modeling*, 60(12):6065–6073, 2020. doi: [10.1021/acs.jcim.0c00675](https://doi.org/10.1021/acs.jcim.0c00675). URL <https://doi.org/10.1021/acs.jcim.0c00675>. PMID: 33118813.
- Wengong Jin, Regina Barzilay, and Tommi S. Jaakkola. Hierarchical generation of molecular graphs using structural motifs. *CoRR*, abs/2002.03230, 2020. URL <https://arxiv.org/abs/2002.03230>.
- M. Kim, M. Jeong, S. Hur, Y. Cho, J. Park, H. Jung, Y. Seo, H. A. Woo, K. T. Nam, K. Lee, and H. Lee. Engineered ionizable lipid nanoparticles for targeted delivery of mRNA therapeutics into different types of cells in the liver. *Science Advances*, 7(9):eabf4398, 2021. doi: [10.1126/sciadv.abf4398](https://doi.org/10.1126/sciadv.abf4398). URL <https://www.science.org/doi/abs/10.1126/sciadv.abf4398>.
- Sunghwan Kim, Paul A. Thiessen, Evan E. Bolton, Jie Chen, Gang Fu, Asta Gindulyte, Lianyi Han, Jane He, Siqian He, Benjamin A. Shoemaker, Jiyao Wang, Bo Yu, Jian Zhang, and Stephen H. Bryant. Pubchem substance and compound databases. *Nucleic Acids Research*, 44(D1):D1202–D1213, 2016. doi: [10.1093/nar/gkv951](https://doi.org/10.1093/nar/gkv951).
- Diederik P. Kingma and Jimmy Ba. Adam: A method for stochastic optimization, 2017. URL <https://arxiv.org/abs/1412.6980>.
- Levente Kocsis and Csaba Szepesvari. Bandit based monte-carlo planning. In *European Conference on Machine Learning*, 2006. URL <https://api.semanticscholar.org/CorpusID:15184765>.
- Byoungjae Kong, Yelee Kim, Eun Hye Kim, Jung Soo Suk, and Yoosoo Yang. mRNA: A promising platform for cancer immunotherapy. *Advanced Drug Delivery Reviews*, 199:114993, 2023. ISSN 0169-409X. doi: <https://doi.org/10.1016/j.addr.2023.114993>. URL <https://www.sciencedirect.com/science/article/pii/S0169409X23003083>.
- Ruvanthy Kularatne, Rachael Crist, and Stephan Stern. The future of tissue-targeted lipid nanoparticle-mediated nucleic acid delivery. *Pharmaceuticals*, 15:897, 07 2022. doi: [10.3390/ph15070897](https://doi.org/10.3390/ph15070897).
- Matt J. Kusner, Brooks Paige, and José Miguel Hernández-Lobato. Grammar variational autoencoder, 2017.
- Bowen Li, Rajith Singh Manan, Shun-Qing Liang, Akiva Gordon, Allen Jiang, Andrew Varley, Guangping Gao, Robert Langer, Wen Xue, and Daniel Anderson. Combinatorial design of nanoparticles for pulmonary mRNA delivery and genome editing. *Nature Biotechnology*, 41(10):1410–1415, 2023. ISSN 1546-1696. doi: [10.1038/s41587-023-01679-x](https://doi.org/10.1038/s41587-023-01679-x). URL <https://doi.org/10.1038/s41587-023-01679-x>.
- Bowen Li, Idris Raji, Akiva Gordon, Lizhuang Sun, Theresa Raimondo, Favour Oladimeji, Allen Jiang, Andrew Varley, Robert Langer, and Daniel Anderson. Accelerating ionizable lipid discovery for mRNA delivery using machine learning and combinatorial chemistry. *Nature Materials*, 23:1–7, 05 2024. doi: [10.1038/s41563-024-01867-3](https://doi.org/10.1038/s41563-024-01867-3).

- Shuai Liu, Qiang Cheng, Tuo Wei, Xueliang Yu, Lindsay T. Johnson, Lukas Farbiak, and Daniel J. Siegwart. Membrane-destabilizing ionizable phospholipids for organ-selective mRNA delivery and CRISPR–cas gene editing. *Nature Materials*, 20(5):701–710, 2021. ISSN 1476-4660. doi: 10.1038/s41563-020-00886-0. URL <https://doi.org/10.1038/s41563-020-00886-0>.
- Shitong Luo, Chence Shi, Minkai Xu, and Jian Tang. Predicting molecular conformation via dynamic graph score matching. In M. Ranzato, A. Beygelzimer, Y. Dauphin, P.S. Liang, and J. Wortman Vaughan, editors, *Advances in Neural Information Processing Systems*, volume 34, pages 19784–19795. Curran Associates, Inc., 2021. URL https://proceedings.neurips.cc/paper_files/paper/2021/file/a45a1d12ee0fb7f1f872ab91da18f899-Paper.pdf.
- Han Han Ly, Simon Daniel, Shekinah K. V. Soriano, Zoltán Kis, and Anna K. Blakney. Optimization of lipid nanoparticles for sarna expression and cellular activation using a design-of-experiment approach. *Molecular Pharmaceutics*, 19(6):1892–1905, 2022. doi: 10.1021/acs.molpharmaceut.2c00032. URL <https://doi.org/10.1021/acs.molpharmaceut.2c00032>. PMID: 35604765.
- Krzysztof Maziarz, Austin Tripp, Guoqing Liu, Megan Stanley, Shufang Xie, Piotr Gaiński, Philipp Seidl, and Marwin Segler. Re-evaluating retrosynthesis algorithms with synthesus. In *NeurIPS 2023 AI for Science Workshop*, 2023. URL <https://openreview.net/forum?id=W5U18rgtpg>.
- Michael J. Mitchell, Margaret M. Billingsley, Rebecca M. Haley, Marissa E. Wechsler, Nicholas A. Peppas, and Robert Langer. Engineering precision nanoparticles for drug delivery. *Nature Reviews Drug Discovery*, 20(2):101–124, 2021. ISSN 1474-1784. doi: 10.1038/s41573-020-0090-8. URL <https://doi.org/10.1038/s41573-020-0090-8>.
- Saeed Moayedpour, Jonathan Broadbent, Saleh Riahi, Michael Bailey, Hoa Thu, Dimitar Dobchev, Akshay Balsubramani, Ricardo Santos, Lorenzo Kogler-Anele, Alejandro Corrochano-Navarro, Sizhen Li, Fernando Montoya, Vikram Agarwal, Ziv Bar-Joseph, and Sven Jager. Representations of lipid nanoparticles using large language models for transfection efficiency prediction. *Bioinformatics (Oxford, England)*, 40, 05 2024. doi: 10.1093/bioinformatics/btae342.
- Xiaolin Pan, Hao Wang, Cuiyu Li, John Zeng Hui Zhang, and Changge Ji. MolGpka: A web server for small molecule pka prediction using a graph-convolutional neural network. *Journal of chemical information and modeling*, 2021. URL <https://api.semanticscholar.org/CorpusID:235798026>.
- Ralph H. Petrucci, William S. Harwood, and F. Geoffrey Herring. *General Chemistry: Principles and Modern Applications*. Prentice Hall, Upper Saddle River, NJ, 8th edition, 2002. ISBN 0-13-014329-4, 978-0-13-014329-7, 0-13-017677-X, 978-0-13-017677-6, 0-13-111673-8, 978-0-13-111673-3. 1 volume (various pagings): illustrations (some color); 26 cm.
- Mikolaj Sacha, Mikolaj Blaz, Piotr Byrski, Pawel Wlodarczyk-Pruszynski, and Stanislaw Jastrzebski. Molecule edit graph attention network: Modeling chemical reactions as sequences of graph edits. *CoRR*, abs/2006.15426, 2020. URL <https://arxiv.org/abs/2006.15426>.
- Ugur Sahin, Katalin Karikó, and Özlem Türeci. mRNA-based therapeutics — developing a new class of drugs. *Nature Reviews Drug Discovery*, 13(10):759–780, 2014. ISSN 1474-1784. doi: 10.1038/nrd4278. URL <https://doi.org/10.1038/nrd4278>.
- Nadine Schneider, Daniel Lowe, Roger Sayle, and Gregory Landrum. Development of a novel fingerprint for chemical reactions and its application to large-scale reaction classification and similarity. *Journal of chemical information and modeling*, 55, 02 2015. doi: 10.1021/acs.jcim.5b00046.
- Marwin H. S. Segler, Mike Preuß, and Mark P. Waller. Towards "alphachem": Chemical synthesis planning with tree search and deep neural network policies. *CoRR*, abs/1702.00020, 2017. URL <http://arxiv.org/abs/1702.00020>.
- Marwin H. S. Segler, Mike Preuss, and Mark P. Waller. Planning chemical syntheses with deep neural networks and symbolic AI. *Nature*, 555(7698):604–610, 2018. ISSN 1476-4687. doi: 10.1038/nature25978. URL <https://doi.org/10.1038/nature25978>.

- Chence Shi, Shitong Luo, Minkai Xu, and Jian Tang. Learning gradient fields for molecular conformation generation, 2021. URL <https://arxiv.org/abs/2105.03902>.
- David Silver, Aja Huang, Chris J. Maddison, Arthur Guez, Laurent Sifre, George van den Driessche, Julian Schrittwieser, Ioannis Antonoglou, Veda Panneershelvam, Marc Lanctot, Sander Dieleman, Dominik Grewe, John Nham, Nal Kalchbrenner, Ilya Sutskever, Timothy Lillicrap, Madeleine Leach, Koray Kavukcuoglu, Thore Graepel, and Demis Hassabis. Mastering the game of go with deep neural networks and tree search. *Nature*, 529(7587):484–489, 2016. ISSN 1476-4687. doi: 10.1038/nature16961. URL <https://doi.org/10.1038/nature16961>.
- David Silver, Julian Schrittwieser, Karen Simonyan, Ioannis Antonoglou, Aja Huang, Arthur Guez, Thomas Hubert, Lucas Baker, Matthew Lai, Adrian Bolton, Yutian Chen, Timothy Lillicrap, Fan Hui, Laurent Sifre, George van den Driessche, Thore Graepel, and Demis Hassabis. Mastering the game of go without human knowledge. *Nature*, 550(7676):354–359, 2017. ISSN 1476-4687. doi: 10.1038/nature24270. URL <https://doi.org/10.1038/nature24270>.
- Martin Simonovsky and Nikos Komodakis. Graphvae: Towards generation of small graphs using variational autoencoders, 2018.
- Stephan T. Stern and Scott E. McNeil. Nanotechnology safety concerns revisited. *Toxicological Sciences*, 101(1):4–21, 2007. ISSN 1096-6080. doi: 10.1093/toxsci/kfm169. URL <https://doi.org/10.1093/toxsci/kfm169>. _eprint: <https://academic.oup.com/toxsci/article-pdf/101/1/4/10976607/kfm169.pdf>.
- Manish Sud, Eoin Fahy, Deirdre Cotter, H. Alex Brown, Edward A. Dennis, Christopher K. Glass, Alfred H. Jr. Merrill, Robert C. Murphy, Christian R. H. Raetz, David W. Russell, and Shankar Subramaniam. LMSD: Lipid maps® structure database. *Nucleic Acids Research*, 2007. PMID: 17098933.
- Richard S Sutton and Andrew G Barto. *Reinforcement learning: An introduction*. MIT press, 2018.
- Kyle Swanson, Gary Liu, Denise B. Catacutan, Autumn Arnold, James Zou, and Jonathan M. Stokes. Generative ai for designing and validating easily synthesizable and structurally novel antibiotics. *Nature Machine Intelligence*, 6:338–353, 2024. doi: 10.1038/s42256-024-00809-7.
- Li Wan, Matthew Zeiler, Sixin Zhang, Yann Le Cun, and Rob Fergus. Regularization of neural networks using dropconnect. In Sanjoy Dasgupta and David McAllester, editors, *Proceedings of the 30th International Conference on Machine Learning*, volume 28 of *Proceedings of Machine Learning Research*, pages 1058–1066, Atlanta, Georgia, USA, 17–19 Jun 2013. PMLR. URL <https://proceedings.mlr.press/v28/wan13.html>.
- Tuo Wei, Yehui Sun, Qiang Cheng, Sumanta Chatterjee, Zachary Traylor, Lindsay T. Johnson, Melissa L. Coquelin, Jialu Wang, Michael J. Torres, Xizhen Lian, Xu Wang, Yufen Xiao, Craig A. Hodges, and Daniel J. Siegwart. Lung SORT LNPs enable precise homology-directed repair mediated CRISPR/cas genome correction in cystic fibrosis models. *Nature Communications*, 14(1):7322, 2023. ISSN 2041-1723. doi: 10.1038/s41467-023-42948-2. URL <https://doi.org/10.1038/s41467-023-42948-2>.
- Anders Wittrup, Angela Ai, Xing Liu, Peter Hamar, Radiana Trifonova, Klaus Charisse, Muthiah Manoharan, Tomas Kirchhausen, and Judy Lieberman. Visualizing lipid-formulated siRNA release from endosomes and target gene knockdown. *Nature Biotechnology*, 33(8):870–876, 2015. ISSN 1546-1696. doi: 10.1038/nbt.3298. URL <https://doi.org/10.1038/nbt.3298>.
- Emily Xu, W. Mark Saltzman, and Alexandra S. Piotrowski-Daspit. Escaping the endosome: assessing cellular trafficking mechanisms of non-viral vehicles. *Journal of Controlled Release*, 335:465–480, 2021. ISSN 0168-3659. doi: <https://doi.org/10.1016/j.jconrel.2021.05.038>. URL <https://www.sciencedirect.com/science/article/pii/S0168365921002728>.
- Yue Xu, Shihao Ma, Haotian Cui, Jingan Chen, Shufen Xu, Fanglin Gong, Alex Golubovic, Muye Zhou, Kevin Chang Wang, Andrew Varley, Rick Xing Ze Lu, Bo Wang, and Bowen Li. AGILE platform: a deep learning powered approach to accelerate LNP development for mRNA delivery. *Nature Communications*, 15(1):6305, 2024. ISSN 2041-1723. doi: 10.1038/s41467-024-50619-z. URL <https://doi.org/10.1038/s41467-024-50619-z>.

Kevin Yang, Kyle Swanson, Wengong Jin, Connor Coley, Philipp Eiden, Hua Gao, Angel Guzman-Perez, Timothy Hopper, Brian Kelley, Miriam Mathea, Andrew Palmer, Volker Settels, Tommi Jaakkola, Klavs Jensen, and Regina Barzilay. Analyzing learned molecular representations for property prediction. *Journal of Chemical Information and Modeling*, 59(8):3370–3388, 2019. doi: 10.1021/acs.jcim.9b00237. Correction published: *J Chem Inf Model*. 2019 Dec 23;59(12):5304–5305. doi: 10.1021/acs.jcim.9b01076.

Xueliang Yu, Shuai Liu, Qiang Cheng, Tuo Wei, Sang Lee, Di Zhang, and Daniel J. Siegwart. Lipid-modified aminoglycosides for mrna delivery to the liver. *Advanced Healthcare Materials*, 9(7): 1901487, 2020. doi: <https://doi.org/10.1002/adhm.201901487>. URL <https://onlinelibrary.wiley.com/doi/abs/10.1002/adhm.201901487>.

A Lipid Building Block Dataset Construction and Selected Examples

We here discuss in detail how the lipid building block dataset construction process is performed and present selected examples of lipid building blocks.

For the ionizable lipid head dataset, we first filter ionizable molecules from the ZINC20 molecule dataset based on the following three criteria:

1. Molecular weight < 500 g/mol.
2. Log P < 0 where the log P is the logarithm (base 10) of the partition coefficient P, which is the ratio of the concentrations of a compound in a mixture of two immiscible phases: typically a hydrophobic solvent and water.
3. Molecules with amine functional groups but not ammonium based molecules.

Since the lipid head building blocks are expected to react with lipid tail building blocks to generate product lipids, we further filter reactive molecules from our ionizable molecule set. We identify reactive molecules by filtering whether or not the molecule contains certain functional groups that participate in common reactions. Specifically, we check whether our candidate molecule contains carboxyl group (i.e., -COOH), hydroxyl group (i.e., -OH), or amine group (i.e., -N or -NH or -NH₂). If the candidate molecule contains any one or more of the target functional groups, we consider the molecule to be reactive. Our filtered reactive ionizable molecule set becomes our ionizable lipid head dataset.

In terms of lipid tail building block dataset, we again filter from the ZINC20 molecule dataset so that our lipid tail building blocks are purchasable. We identify a lipid tail building block if the molecule is similar to an actual lipid tail (i.e., the tail component of an existing lipid). We use a lipid dataset sourced from the LipidMaps database and the SwissLipid database [Sud et al., 2007, Aimo et al., 2015]. Leveraging the Lipid Analyzer, an implemented toolkit for lipid tail extraction, we extract lipid tails from this lipid dataset. The Lipid Analyzer finds the lipid head for a given lipid, we then extract lipid tails by removing the head substructure. For a given molecular structure, the algorithm first recognizes ring structures. For all possible arrangements of the rings, the algorithm then removes carbon atoms that are not near any hydrophilic atom and not forming any ring. If only one substructure remains after the operation, and if the log P value of this substructure is low enough, this substructure will be identified as the lipid head. It's then easy to extract tail substructures by removing the head substructure.

We then conduct a similarity comparison to filter those molecules from the ZINC20 dataset that are similar to a real lipid tail. The similarity is measured by the Graph Edit Distance (GED) between two molecular structures, quantifying the minimum number of operations required to transform one graph into another. We only select molecules that has GED value smaller or equal to 1 with a real lipid tail. Meanwhile, we also consider the similarity between molecular fingerprint representations, Daylight fingerprint and Extended Connectivity Fingerprint 4 (ECFP4) are considered. The resulting molecules make up our lipid tail building block dataset.

Selected examples of our lipid head building blocks with different functional groups are shown in Figure 5. The first row presents examples with no carboxyl group, one hydroxyl group, and two amine groups; the second row presents examples with one carboxyl group, no hydroxyl group, and one amine group; the third row presents examples with two carboxyl groups, no hydroxyl group, and one amine group. Note that we only consider independent amine groups that are linked to only simple carbon atoms. For example, in the first example of the first row, we find a secondary amine group (i.e., -NH) linked to a carbonyl group (i.e., C=O, a carbon atom double-bonded to an oxygen atom). The linkage with the carbonyl group forms a more complicated substructure, which influences the reactive performance of the amine group. We therefore exclude this secondary amine group when counting our target functional groups. Similarly, the nitrogen-nitrogen bond (i.e., N-N) which appears in a five-membered nitrogen-containing ring influences the reactive property of the nitrogen, and we also exclude these nitrogen atoms when counting the occurrence of amine functional groups.

Figure 6 shows selected examples of lipid tail building blocks. As we can see, a lipid tail usually consists of a carbon chain and a functional group. The functional group may be hydroxyl group, amine group, or a halogen atom.

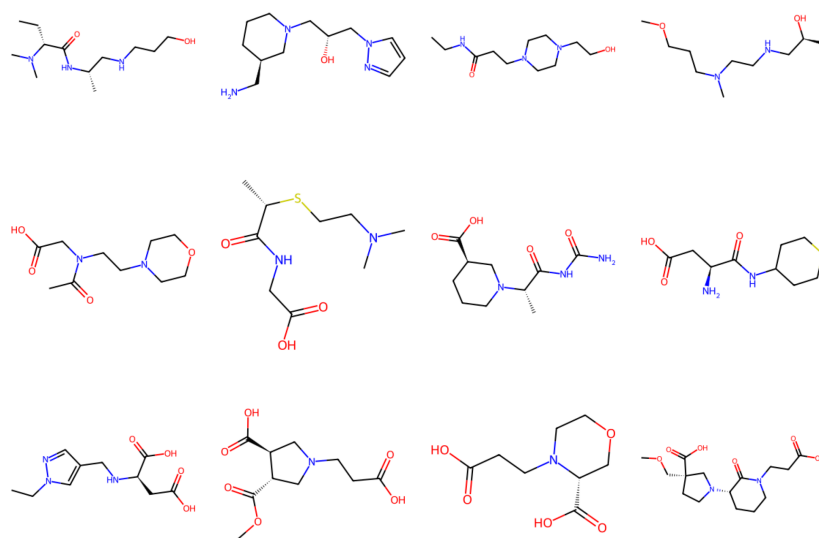


Figure 5: Selected examples of lipid head building blocks.

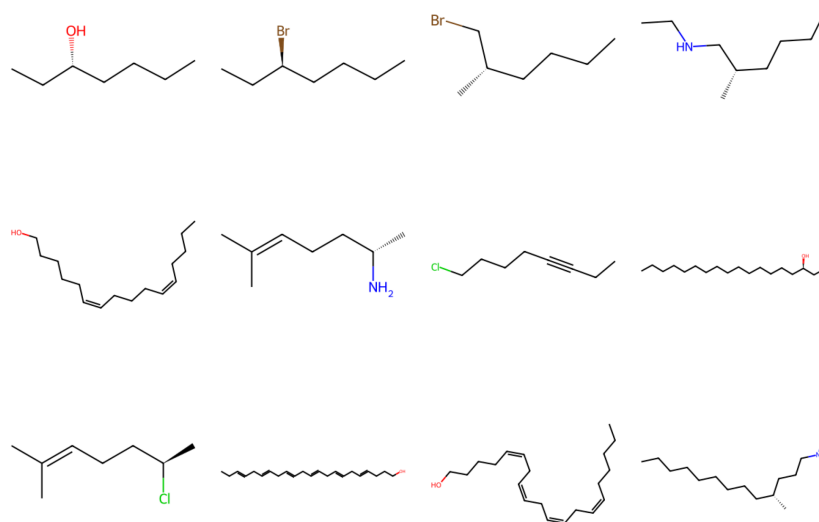


Figure 6: Selected examples of lipid tail building blocks.

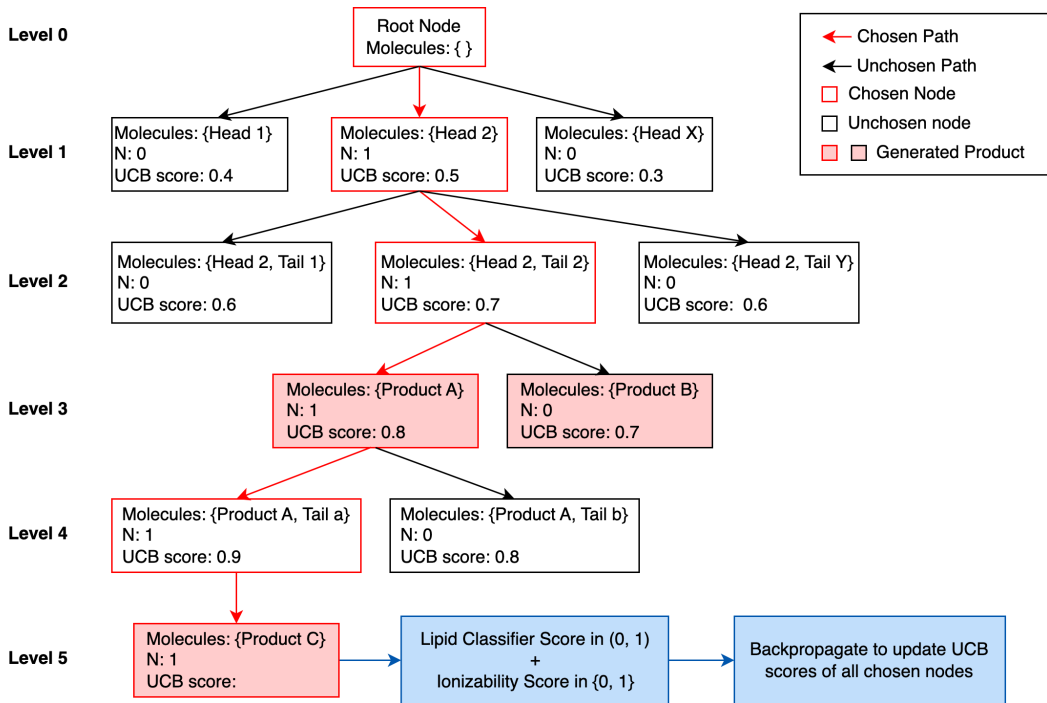


Figure 7: SyntheMol for lipid generation.

B SyntheMol for Lipid Generation

Figure 7 illustrates a typical simulation of the MCTS process in our lipid generation. In the search tree, each node stores crucial statistics: the molecules represented by the node, the node’s visit count N , and the Upper Confidence Bound (UCB) score. The UCB score guides the node selection process using the UCB action selection criterion [Sutton and Barto, 2018, Kocsis and Szepesvari, 2006]. The UCB score combines an action value Q , which represents the average of the total action values W (i.e., the sum of the values of the final products passing through the node), with an upper confidence term U . This term is defined as $U(\text{node}) \propto \frac{P(\text{node})}{1+N(\text{node})}$, where $P(\text{node})$ indicates the property scores assigned to the node. The complete formula for the UCB score is as follows:

$$UCB_score(\text{node}) = Q(\text{node}) + U(\text{node}) \quad (4)$$

$$= \frac{W(\text{node})}{N(\text{node})} + c \cdot P(\text{node}) \cdot \frac{\sqrt{1+n}}{1+N(\text{node})} \quad (5)$$

where n is the total visit count of all nodes at the same level as the target node and c is a constant exploration parameter controlling the level of exploration. Note that the P value is the property score calculated by our property predictors. When a node represents multiple molecules, the P value for that node is computed as the average of the property scores for each constituent molecule.

It is important to note that the assignment of property scores to nodes at non-terminal levels—representing either building block molecules or intermediates—may initially seem illogical, as direct evaluation of these entities’ properties does not typically yield meaningful insights. However, this approach does not compromise the long-term efficacy of the algorithm. Over time, as more product molecules are synthesized and action values refined, the utility of early-stage evaluations is validated. SyntheMol’s findings corroborate this approach, demonstrating that despite low scores of individual building blocks, the synthesized molecules often exhibit significantly higher scores, which are effectively identified by MCTS, highlighting its capability to uncover promising molecules overlooked by simpler scoring methods [Swanson et al., 2024].

The MCTS algorithm commences at a root node (level 0), an empty initial node, which is then expanded with child nodes representing available lipid head building blocks defined within our chemical space (level 1). Each child node receives an UCB score, with the node exhibiting the highest

UCB score selected for further expansion. This selected node is expanded to include a lipid tail building block, generating second-level nodes where each combination represents potential reactants (level 2).

Subsequently, the node with the highest UCB score from level 2 is selected and expanded. This stage differs from prior expansions in that it now entails actual chemical reactions between the two building blocks within the node. The resulting third-level nodes embody all conceivable products predicted by forward reaction mechanisms (level 3). This iterative expansion continues until either a valid final product (i.e., a two-tail lipid in our case) is synthesized, or further reactions become untenable with the existing building blocks in our dataset.

Upon terminating the simulation with a valid final product, the synthesized molecule is assessed using our property predictors. The resultant property value is then backpropagated to update the UCB scores along the simulated pathway. For analysis purpose, we meticulously document all products, including intermediates, generated during each simulation.

C Algorithm of Guided Monte Carlo Tree Search for Lipid Generation

We define a Node class to represent the nodes appeared in the tree search. The Node class has the following attributes:

- `state`: Stores the SMILES representation of the molecule represented by this node.
- `N`: A visit count of the node, initialized to zero.
- `P`: The prior probability assigned based on predictions from a policy network.
- `W`: The cumulative value sum, representing the total assessed value of this node's state.
- `children`: A dictionary to hold child nodes, with the keys of the dictionary to be actions (i.e., the next building blocks to select) and the values to be corresponding child nodes.

Algorithm 1 Policy Network Guided MCTS

Require: Product(): reaction predictor
Require: PropertyScore(): property score predictor
Require: SearchProbability(): search probability calculator

- 1: $f_\theta \leftarrow$ randomly initialized neural network with parameter θ
- 2: $\lambda \leftarrow$ regularization constant
- 3: $\alpha \leftarrow$ learning rate
- 4: $c \leftarrow$ exploration weight
- 5: $D = \emptyset$

- 6: **for each iteration do**
- 7: **for each play do**
- 8: $S_0 \leftarrow$ empty root state
- 9: $D_{play} \leftarrow$ MCTS(S_0)
- 10: $D = D \cup D_{play}$
- 11: **end for**
- 12: **for each epoch do**
- 13: Train f_θ using D
- 14: **end for**
- 15: Reset $D = \emptyset$
- 16: **end for**

- 17: **function** MCTS($root_state$)
- 18: Initialize $root_node$ with $root_state$
- 19: EXPAND($root_node$)
- 20: $generation = \emptyset$
- 21: **for each simulation do**
- 22: $leaf_node, search_path \leftarrow$ SELECT($root_node$)
- 23: **if** $leaf_node$ is two-tail lipid **then**
- 24: $v =$ PropertyScore($leaf_node$)
- 25: Add $search_path$ to $generation$
- 26: **else**
- 27: EXPAND($leaf_node$)
- 28: $v \leftarrow$ ROLLOUT($leaf_node$)
- 29: **end if**
- 30: BACKPROPAGATE($v, search_path$)
- 31: **end for**
- 32: Write $generation$ to log file
- 33: **return** visit counts of all state-action pairs
- 34: **end function**

Algorithm 2 Select Function in MCTS

- 1: **function** SELECT($root_node$)
- 2: $search_path = []$
- 3: $node \leftarrow root_node$
- 4: **while** $node.children$ is not empty **do**
- 5: $selected_action = \arg \max_a$ UCB_SCORE($node, node.children[a]$)
- 6: $node \leftarrow node.children[selected_action]$
- 7: Add $node$ to $search_path$
- 8: **end while**
- 9: Update $node.state$ with Product($node.state, selected_action$)
- 10: **return** $node, search_path$
- 11: **end function**

Algorithm 3 Expand Function in MCTS

```
1: function EXPAND(node)
2:    $A(\textit{node}) \leftarrow \text{NEXT\_BUILDING\_BLOCKS}(\textit{node})$ 
3:    $P(\textit{node}, \cdot) = f_{\theta}(\textit{node.state}, A(\textit{node}))$ 
4:   for  $a$  in  $A(\textit{node})$  do
5:     Initialize child_node with  $P(\textit{node}, a)$ 
6:      $\textit{node.children}[a] = \textit{child\_node}$ 
7:   end for
8: end function
```

Algorithm 4 Backpropagate Function in MCTS

```
1: function BACKPROPAGATE( $v$ , search_path)
2:   for node in search_path do
3:      $\textit{node.N} \leftarrow \textit{node.N} + 1$ 
4:      $\textit{node.W} \leftarrow \textit{node.W} + v$ 
5:      $\textit{root\_node.N} \leftarrow \textit{root\_node.N} + 1$ 
6:   end for
7: end function
```

Algorithm 5 Rollout Function in MCTS

```
1: function ROLLOUT(node)
2:   while node.state is not two-tail lipid do
3:      $A(\textit{node}) \leftarrow \text{NEXT\_BUILDING\_BLOCKS}(\textit{node})$ 
4:     return 0 if  $A(\textit{node})$  is empty
5:      $a \leftarrow$  a random choice from  $A(\textit{node})$ 
6:     node  $\leftarrow$  new node with Product(node.state,  $a$ )
7:   end while
8:   return PropertyScore(node)
9: end function
```

Algorithm 6 UCB Score Calculation Function in MCTS

```
1: function UCB_SCORE(parent_node, child_node)
2:   if  $\textit{child\_node.N} = 0$  then
3:      $Q = 0$ 
4:   else
5:      $Q = \frac{\textit{child\_node.W}}{\textit{child\_node.N}}$ 
6:   end if
7:    $U = c \cdot \textit{child\_node.P} \cdot \frac{\sqrt{\textit{parent\_node.N}}}{\textit{child\_node.N} + 1}$ 
8:   return  $Q + U$ 
9: end function
```

Algorithm 7 Get Action Space Function in MCTS

Require: *max_expand_num* a pre-determined number

```
1: function NEXT_BUILDING_BLOCKS(node)
2:   if node is empty node then
3:      $A(\textit{node}) \leftarrow \textit{max\_expand\_num}$  random samples from head search space
4:   else
5:     reactive_tail_set  $\leftarrow$  tails which can react with node.state
6:      $A(\textit{node}) \leftarrow \textit{max\_expand\_num}$  random samples from reactive_tail_set
7:   end if
8:   return  $A(\textit{node})$ 
9: end function
```

D Policy Network Training

As is mentioned before, the visit counts of all state-action pairs that appear in the tree search are recorded to be the training data of the policy network. However, the search data we collect are highly imbalanced in the sense that there will be a lot more state-action pairs in later levels. The number of state-action pairs from the first level (i.e., when state is the empty state and actions are the chosen head building blocks) is very limited, being the number of different head building blocks that are expanded by the root node. Meanwhile, search data from later levels will be very sparse in the sense that the majority of the state-action pairs will have zero visit count. In order to better utilize our limited data, we propose a customized method for training the policy network.

Let $f(s, a)$ denote the naive policy network output (before softmax) for the state-action pair (s, a) , $p(s, a)$ denote the corresponding predicted prior (which will be used in the UCB score calculation), and $\pi(s, a)$ be the search probability. We here adopt the search probability definition as proposed in the AlphaZero algorithm [Silver et al., 2017].

$$p(s, a_1) = \frac{e^{f(s, a_1)}}{\sum_a e^{f(s, a)}} \quad (6)$$

$$\pi(s, a_1) = \frac{N(s, a_1)^{\frac{1}{\tau}}}{\sum_a N(s, a)^{\frac{1}{\tau}}} \quad (7)$$

where τ is a temperature parameter controlling the level of exploration. When τ tends to infinity, the search probability is the same as random selections. When τ is small, say, when $\tau = 1$, the search probability strictly follows the actual visit count distribution. The objective of the policy network training is to maximize the similarity of $p(s, a)$ and $\pi(s, a)$.

Now, suppose we take two state-action pairs, (s, a_1) and (s, a_2) , at a time. We apply the log-ratio and get:

$$\log \frac{p(s, a_1)}{p(s, a_2)} = f(s, a_1) - f(s, a_2) \quad (8)$$

$$\log \frac{\pi(s, a_1)}{\pi(s, a_2)} = \frac{1}{\tau} \log N(s, a_1) - \frac{1}{\tau} \log N(s, a_2) \quad (9)$$

The previous objective is equivalent to maximize the similarity of $f(s, a_1) - f(s, a_2)$ and $\frac{1}{\tau} \log N(s, a_1) - \frac{1}{\tau} \log N(s, a_2)$.

We therefore customize the loss function to be the error between $f(s, a_1) - f(s, a_2)$ and their corresponding $\frac{1}{\tau} \log N(s, a_1) - \frac{1}{\tau} \log N(s, a_2)$, for any two state-action pairs, (s, a_1) and (s, a_2) . This can be considered as a regression problem, MAE or MSE loss may be applied.

E Selected Examples of Synthesis Planning

Figures 8 and 9 give two examples of our generated ionizable lipids with their corresponding synthesis paths. Note that these synthesis paths have been validated by the retrosynthesis tool Syntheseus [Maziarz et al., 2023]. In the figures below, the blue nodes represent product molecules (i.e., intermediate product or final product) and the green nodes represent building block molecules (i.e., lipid head building block or lipid tail building block).

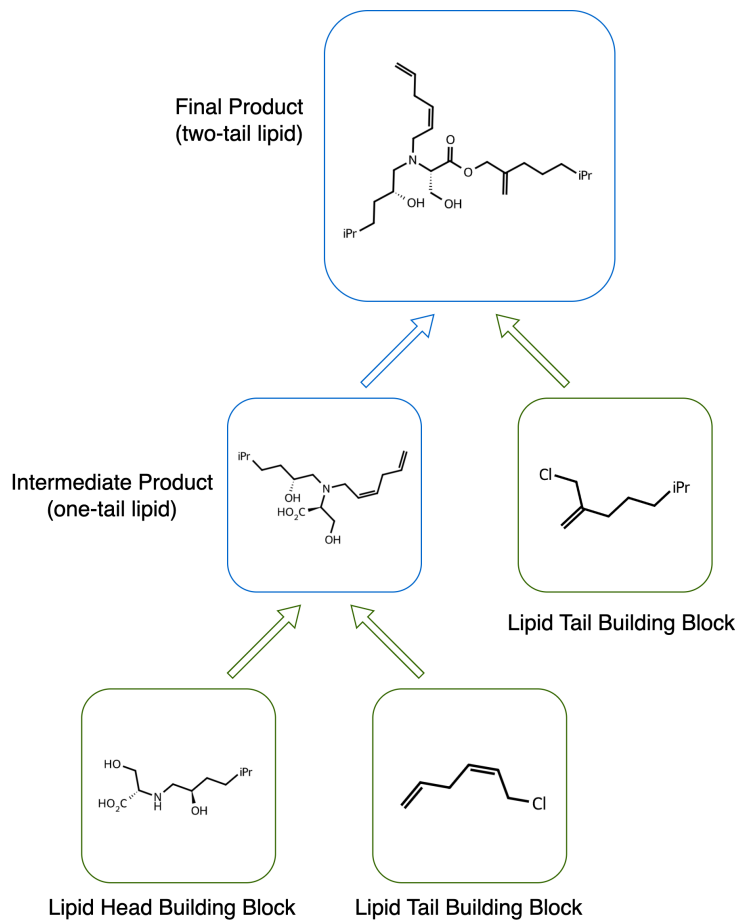


Figure 8: Example 1 of generated ionizable lipid with synthesis path.

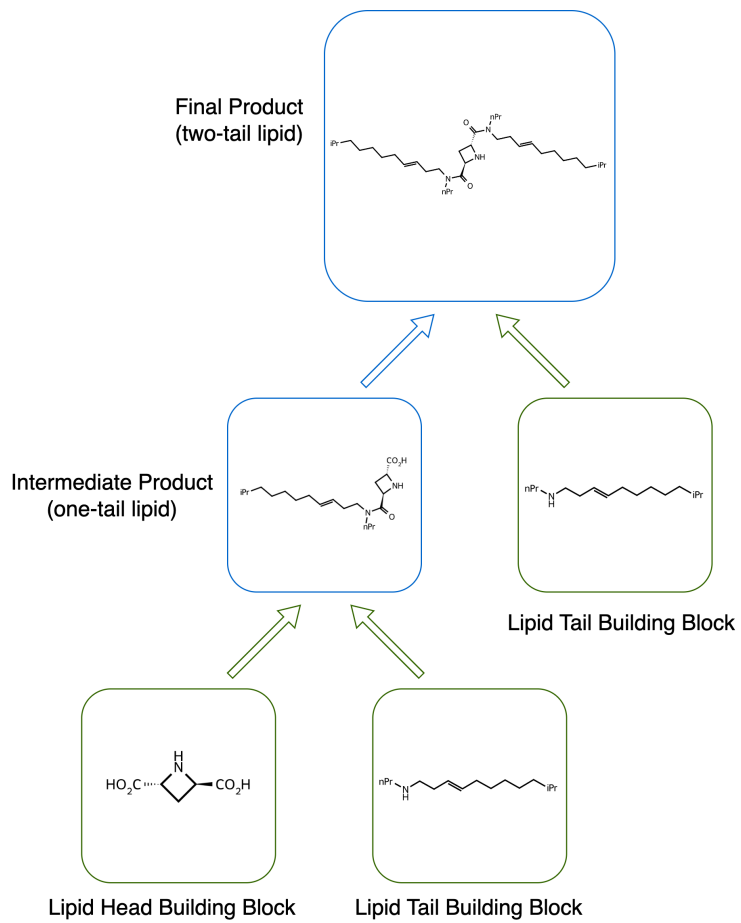


Figure 9: Example 2 of generated ionizable lipid with synthesis path.